

Pressure control of rolling-seal tape spring actuators

Curtis Sparks, Tommy Jin, Nick Gravish, *Member, IEEE*,

Abstract—Tape spring mechanisms are useful in soft robotics for their ability to extend long distances and exhibit both high strength and high flexibility. In this work we introduce a new tape-spring based actuator concept that uses internal fluidic actuation to achieve: 1) stiffness control of tape-spring beams, and 2) shape modulation of a length-constrained tape-spring actuator. This concept relies on the ability of sealed tape-springs to form a rolling pressure seal when the mechanism is bent, and thus through differential pressure control across the bend we can reconfigure the actuator shape. We first describe the fabrication methods for sealed tape-spring actuators and then characterize their mechanical and hydraulic properties. Three-point bend tests of open and hydraulically sealed tape-spring beams enable us to determine how fluid pressure influences mechanical stiffness. We measured the sealing characteristics of the rolling bend seal by measuring mass-flow through the bend at different input pressures. These characterization experiments allowed us to build a length-constrained actuator which can change stiffness, and actuate through differential pressure control. Fluidic control of rolling-seal tape spring actuators presents new opportunities for using tape-spring mechanisms in situations where electromagnetic actuation may be unfavorable or infeasible.

I. INTRODUCTION

Tape springs have many properties that make them useful in soft robotics as their curved structure allows them to extend to significant distances while remaining stiff and lightweight. For these reasons tape springs are often used for lightweight hinges [1] and for supports in outer space [2], [3]. These properties have also been used to create multiple types of soft robots, including; swimming robots [4], extensible manipulators [5], deployable robots [6], and robots that can climb or pull themselves along the ground [7]. However, all of these robots rely on motors to provide motion, which can be a problem in situations where there are limitations on space or weight, or in applications where metal components are undesirable.

Some soft robots have shown to produce motion without motors by using pressure control or volume change through hydraulic or pneumatic actuation. Examples of pneumatic soft robots include PneuNets [8] and artificial muscles [9] which produce bending and shortening motions respectively when a pneumatic pressure is applied. Pneumatic soft robots have been used to create humanlike hands [10], growing continuum robots [11], crawling robots [12], and modular robots [13]. Examples of hydraulic soft robots include underwater walking robots [14], artificial muscles [15], grasping hands [16], and biologically inspired robots [17]. All of these

mechanisms create motion without using motors. In order to use hydraulic or pneumatic power, there needs to be a sealed space for the pressure or volume change to act on.

Two surfaces pressed together in a curve can form an airtight seal and create motion when pressurized. This is commonly seen in the new years party horn, a coiled ribbon which extends when blown into. This property was also shown in an extending soft robot [18]. This paper demonstrates that a similar structure can be created by placing two tape springs together with opposite curvature and buckling them. Where the two tape springs buckle, they flatten out and press together in a rolling joint that can be moved along the length of the tape springs. We demonstrate that this rolling joint is also an airtight seal, separating the tape spring beam into two separate chambers.

This work presents a novel soft robotic mechanism called the rolling-seal tape spring actuator (RSA). The RSA uses the rolling joint formed by buckling a tape spring as both a seal and a joint for hydraulic actuation. This movable seal allows for motion and actuation without a motor. In section II of this paper we introduce the construction and kinematics of the RSA. Section III examines the buckling strength and pressure resistance of the RSA through a series of tests and demonstrations.

II. DESIGN OF ROLLING-SEAL TAPE SPRING ACTUATORS

A. Fabrication

The rolling-seal actuator is designed to be water tight and easy to construct. The base of the rolling-seal actuator is two lengths of tape spring placed so the sides of their concave curves touch (Fig. 1a). The “oval” cross-section of this structure provides stiffness to axial and transverse loads, while maintaining the ability to easily buckle and bend along the length. The hollow cavity formed by the two tape springs is sealed with duct tape to create a pressure-tight cavity. The duct tape wrapping holds the tape springs in place and prevents fluid from leaking round the outside or corners of the seal.

When the tube is bent, a rolling joint is formed where the two tape springs flatten out and press against each other (Fig. 1b). This bend location forms a rolling pressure seal that can be relocated by moving the bend along the tape. By controlling the volume of the beams on the left and right sides of the rolling seal, the rolling-seal can be relocated. The actuator concept we develop uses a fixed-length tape-spring beam with free rotational joints at the base.

Initially, the ends of the tube were sealed by a 3D printed cap with connecting tubing that is sealed in place with epoxy (Fig. 1). However, this design was prone to leaking. It was

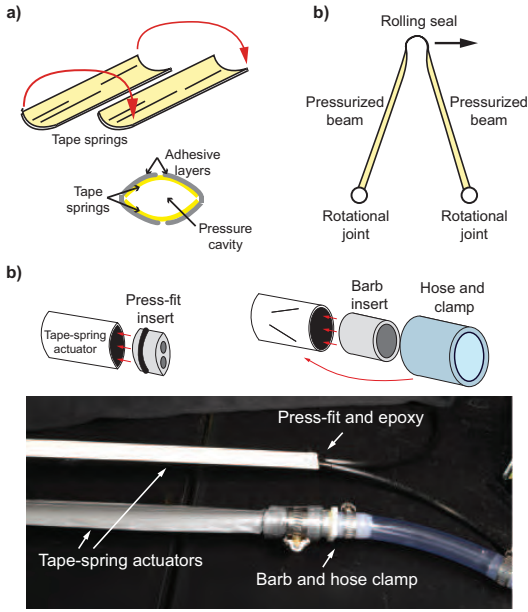


Fig. 1. Tape-spring rolling-seal actuator fabrication. a) Two lengths of tape-springs are laminated together with their concave sections pointing towards each other. A pressure sensitive adhesive is applied along both seams of the two tape-springs to create a sealed cavity. b) Two methods were used to connect rolling-seal actuators with hydraulic or pneumatic pressure sources: a 3D printed insert with O-ring (left), and a hose-barb insert with surrounding hose and clamp. Image: Upper tape is original design with 3D printed endcap sealed with epoxy. Lower tape is improved design using tubing, barbed fitting, and metal collar.

difficult to form an initial seal and would develop leaks during testing. The 3D printed cap was later replaced by putting the end of the tape in a 5/8 inch inner diameter tube and putting a 5/8 inch barbed tube fitting inside the tape and then sealing the assembly together by tightening a metal collar around it. This provided a much more successful seal, however it had the effect of creating a circular cross-section at the base of the actuator.

We used both hydraulic and pneumatic pressure sources for the rolling-seal actuator. Push-to-connect tubing was connected to a pressurized air source through a pressure regulator (Max pressure 160psi). Hydraulic actuation used two 150mL syringes which were connected to each side of the rolling-seal actuators pressurized beams. These syringes were manually actuated to perform bi-directional movement of the actuator.

B. Actuator kinematics and statics

To begin our analysis of tape-spring rolling-seal actuators we first introduce the kinematics of our fixed-length design. The actuator has a kinematic structure consistent with a series of rotational (R) and prismatic (P) joints configured from the fixed base as an RPRPR mechanism (Fig. 2). Despite the five rotation/prismatic joints, the mechanisms has only a single degree of freedom because of two sets of constraints: 1) the total length is constrained to be $l_1 + l_2 = L$, and 3) the actuator is formed into a triangle which geometrically constrains the allowable angles of the three rotational joints.

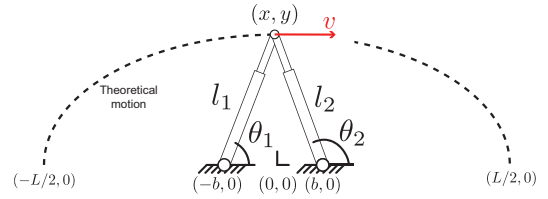


Fig. 2. Kinematic representation of a tape-spring rolling-seal actuator. The total length is constrained and the angles are determined by the side-length and base-separation distance. The theoretical motion of the rolling-joint tip is along an ellipse with the two rotational bases at the ellipse's foci.

Due to the constraint of the overall actuator length, the left and right beams change length differentially with one shortening by the exact amount the other lengthens. This constraint is reminiscent of the simple construction of an ellipse which can be drawn by placing a string at two points (the ellipse foci) and tracing with a pencil the line formed when the strings are taut. Thus, the kinematic configuration and constraints on our actuator yield a theoretical workspace consisting of an elliptical path centered about the midpoint between the base rotational joints with semi-major axes $L/2$ and semi-minor axes $\sqrt{(L/2)^2 - b^2}$. The total length is fixed at L and control of either l_1 or l_2 individually may be used to completely control the shape of the actuator.

To analyze the force production of the actuator we here describe the differential kinematics of the system. The loop constraints on the actuator along the x and y directions produce two equations that relate the angles and lengths

$$l_1 c_1 - l_2 c_2 - 2b = 0 \quad (1)$$

$$l_1 s_1 - l_2 s_2 = 0 \quad (2)$$

(where c_1 denotes $\sin(\theta_1)$). Isolating the θ_2 terms on the left hand side, substitution of the relation $l_2 = L - l_1$ into both equations, and then squaring each equation allows for all θ_2 terms to be removed yielding

$$(L - l_1)^2 + 2bl_1 c_1 - 4b^2 = 0 \quad (3)$$

This equation allows for solving the solution of θ_1 , and subsequently θ_2 if given a l_1 . Furthermore, the time derivative of this equation can be used to solve for the relations between \dot{l}_1 (our control input) and $\dot{\theta}_1, \dot{\theta}_2$. Through construction of the standard differential kinematics of the left-side actuator, and solving for θ_1 and $\dot{\theta}_1$ as functions of l_1 and \dot{l}_1 yields the standard Jacobian relationship

$$\begin{bmatrix} \dot{x} \\ \dot{y} \end{bmatrix} = J(l_1) \dot{l}_1 \quad (4)$$

For space and practical purposes in this work we numerically solve for the function $J(l_1)$.

III. TESTING AND EVALUATION

A. Buckling Strength

One of the proposed benefits for creating a hydraulically actuated mechanism is that it will be more resistant to buckling than an unsealed version. A leg filled with incompressible fluid could be stronger and more resistant to

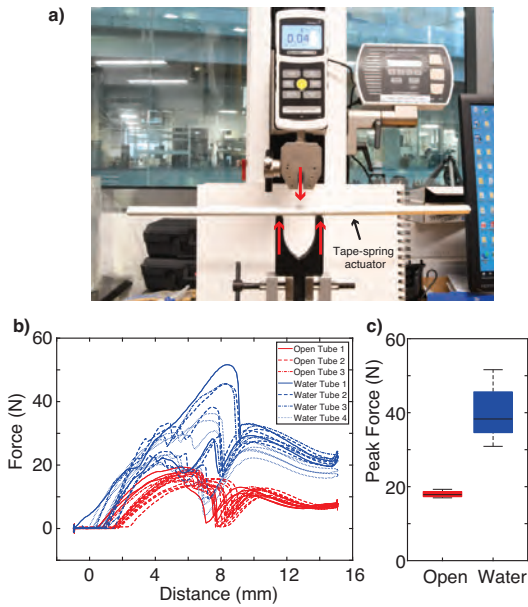


Fig. 3. Three point bending setup using a mark 10 force measurement machine. a) Photo of experiment setup with uncapped open actuator. b) Force vs displacement measurements for three point bending tests. c) Peak force comparison of open tapes and water filled tapes.

buckling as the fluid filling the chamber of the leg would need to be displaced for the buckling to occur.

This was tested by performing a three point bending test comparing tapes with open ends and tapes with capped ends which were filled with water. For each test, the specimen was placed on a set of two points spaced 50mm apart and a third point was pressed down in the center using a Mark 10 model DC4050. The center point was moved 15mm down from where it contacted the tape and throughout the motion the measured force on the center point was recorded. The center point was then raised back out of the way and the specimen was moved to test another point along its length. Three measurements were taken on each specimen. In some cases the test on a particular specimen had to be stopped early as it was damaged and could not be tested again, this was common with the water filled tapes which would develop a leak and lose water. This test was repeated seven times with three uncapped tapes open to the air, and four sealed and water filled tapes.

The water filled tapes performed significantly better in the three point bending test (Fig. 3). The median value of the peak buckling force for the water filled tapes was more than double the median value of the peak buckling force for the open tapes, at 38.3 and 17.8 newtons respectively.

B. Bend Sealing

The actuation method of driving the rolling-seal actuators by hydraulic or pneumatic power assumes that when the rolling joint is formed and the two tapes flatten against each other that forms a pressure seal. That seal prevents fluid from moving between the two legs of the actuator. This was tested by applying an air pressure to one leg of the rolling-

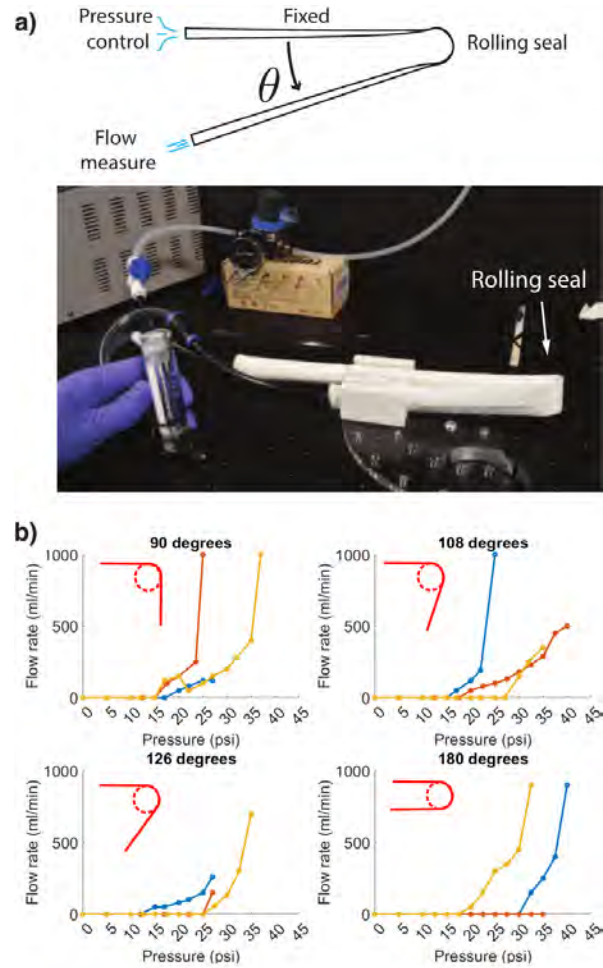


Fig. 4. a) Setup for bend sealing test. Tape is held in place by 3D printed clamps locked into a laser cut base plate at specific angles. One side of the tape is attached to a pressure regulator. The other end is attached to an airflow sensor to measure flow through the joint. b) Measured flow through the rolling seal vs applied pressure at different bend angles.

seal actuator and measuring the airflow out of the other side.

A rolling-seal actuator with one tube on each end was held in position with an angle locking mechanism consisting of a laser cut acrylic baseplate and two pairs of 3d printed clamps. The angle mechanism would hold the two legs of the rolling-seal actuator at a specific angle with 6 steps of even distribution from 90 degrees to 180 degrees bend angle. One end of the rolling-seal actuator was attached to a pneumatic regulator and the other was connected to an airflow meter. The rolling-seal actuator was locked to an angle and the pressure was increased until an airflow could be measured through the opposite leg of the rolling-seal actuator. Once a high airflow rate was observed, the pressure was lowered to zero. Then the angle was changed and the bend was moved to another point on the tape to avoid measuring from damaged areas. This process was started at 90 degrees for each specimen and was increased towards 180 degrees. However, most rolling-seal actuators would fail catastrophically before reaching the 180 degree bend angle. The tapes would begin to leak or otherwise deform in a way

that made further testing impossible when subjected to higher pressures. To get a better measurement of the sealing force at higher angles, two tapes were started at 180 degrees before doing any other tests.

Below 15psi there is little to no airflow through the sealing joint (Fig. 4). Above 15psi the rolling-seal actuator starts to allow air flow through the joint at varying pressures and increases with an increase in pressure. There was little dependence of the bend angle on the failure pressure that leakage occurred at. For all bend angles and experiments we found that 15psi was a suitable pressure to repeatedly apply to the rolling-seal actuator without leakage or failure. Therefore the rolling joint of the actuator can be treated as a seal and the two legs can be treated as independent chambers.

When the rolling seal did fail it was often catastrophic resulting in total failure of the actuators pressure seal. Failure occurred through tearing of the adhesive layer surrounding the inner tape-springs, and often occurred near the rolling seal location because of the high strain induced by the generation of the rolling seal cross-section.

C. Force Transmission

One of the predicted benefits of using hydraulic propulsion was the ability to measure force and contact through pressure. To evaluate this theory, a force test was performed. A force torque sensor was placed along the elliptical path described in section II.B with $b = 228\text{mm}$ and $L = 457\text{mm}$. The position of the sensor along the ellipse was defined by the angle between a line drawn through the right basepoint and the line connecting both basepoints. The rolling-seal actuator was mounted on the basepoints with a set of rotating blocks. The rolling-seal actuator was filled with water and attached to an air pressure regulator. The chamber opposite the force sensor was pressurized causing the rolling-seal actuator to push into the force sensor. The force measured by the load cell was recorded and then the pressure was increased. The pressure increase continued until it reached 15psi. The test was performed at three different angles; 30° , 45° , and 60° . Three measurements were taken at each angle. The rolling-seal actuator produced an average force above 3N at 15psi.

D. Actuation Tests

The rolling-seal actuator consists of two chambers of changing volume connected together. Therefore it was predicted to behave similarly to a hydraulic piston; where a change in the volume of fluid would produce a motion and fluid input on one side would produce a corresponding fluid expulsion on the other.

A rolling-seal actuator with an input and output tube on both ends was mounted vertically on a metal plate with both ends free to rotate. The rolling-seal actuator was arranged so that the short side of the actuator was vertical and the rolling joint was hanging below the first mounting point. Both sides were filled with water by putting water in the input tube until it overflowed through the output tube. A water filled syringe was attached to the input of the short side to drive motion

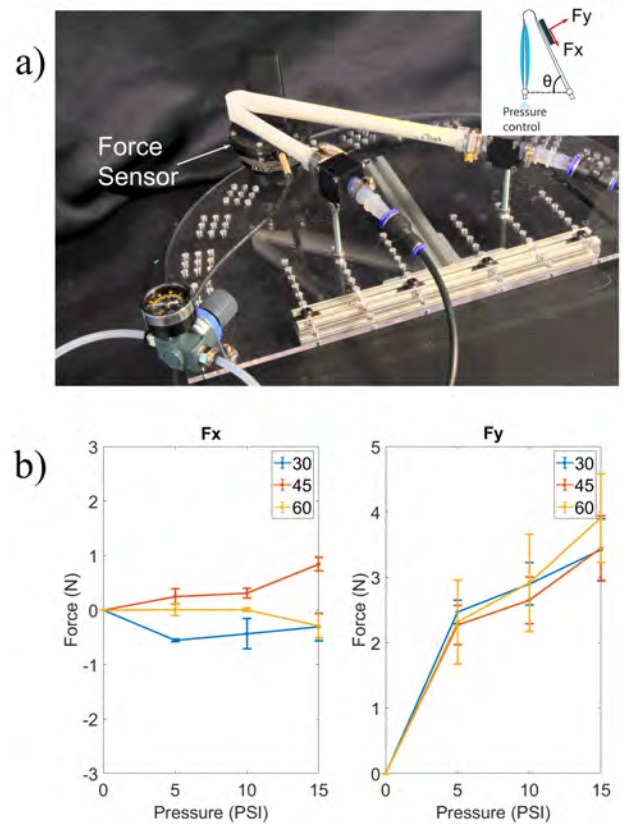


Fig. 5. Force measuring experiment setup. a) Photo of force measurement setup showing rolling-seal actuator filled with water and mounted on rotating blocks. The left side is pressurized with a regulated air pressure. Force output is measured by a force torque sensor. b) Measured force at different pressures and angles. F_x is parallel to the unactuated arm, F_y is perpendicular to the unactuated arm.

by inputting more water. The output of the long side was placed in a beaker to measure any water flowing out of the system.

The initial volume of the syringe was recorded. Then force was then applied to the plunger of the syringe, putting water into the system. The pressure continued until the rolling joint of the rolling-seal actuator had moved to below the second mounting point. The system was then allowed to settle for a few seconds and when all change had stopped, the final volume of the syringe and volume of expelled water in the beaker were recorded.

The rolling joint of the tape traveled about 200mm in each test. The change in syringe volume from start to end of test and volume of expelled water in the beaker averaged 25 and 33 ml respectively. Before the increase in volume causes the joint to move, the cross section of the rolling-seal actuator deforms to be more circular. The un-deformed cross section of the rolling-seal actuator is two symmetric convex curves 23 mm wide and 5.5mm at their tallest point. This produces a cross sectional area of 194mm^2 . A circle with a circumference equal to the perimeter of the un-deformed cross section has an area of 221mm^2 . The change in area due to the deformation is 27mm^2 . After the joint has moved,

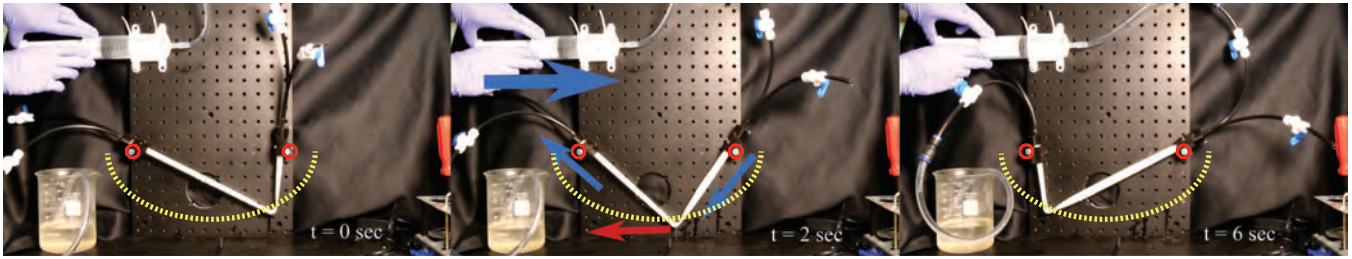


Fig. 6. Unidirectional motion test with rolling-seal actuator mounted on a vertical plate using hydraulic actuation. Blue arrows show the flow of water, red arrow indicates motion of the rolling joint due to volume change. Yellow dashed line shows the predicted trajectory from measurements of total tape length and pivot separation.

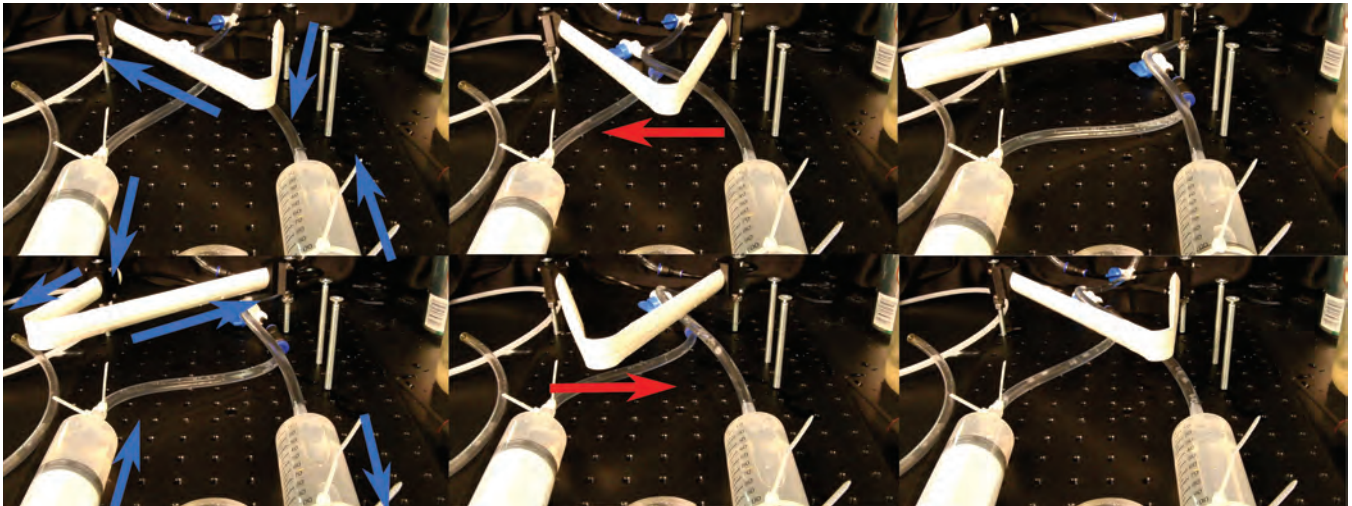


Fig. 7. Bidirectional motion of rolling-seal actuator under hydraulic control driven by two syringes. Blue arrows show direction of water flow, red arrow shows motion of rolling joint.

the driving leg is about 300mm long. The extra volume in the leg due to deformation is 8ml. When the force on the plunger is removed, the cross section returns to the convex lens shape and the extra water is returned to the plunger as the pressure decreases.

A final demonstration was performed to showcase the abilities of the actuator (Fig- 8). The actuator started in a vacuumed state, where all air and water had been pulled out from between the tapes. This leaves the actuator in a flexible state where it can be easily manipulated or bent out of the plane. The vacuum was released and the actuator was filled with water, forming a stiff mechanism. Then using hydraulic control provided by manually driven syringes, the actuator pushed over a bottle of water and returned to its initial position. After knocking over the bottle, the water was pulled out of the actuator and the actuator returned to its flexible state.

IV. DISCUSSION AND CONCLUSION

This work investigated using hydraulic and pneumatic actuation to improve performance in tape spring mechanisms. An actuator was created by wrapping a pair of tape springs in a waterproof layer and sealing the ends. The water filled tape mechanisms demonstrated higher buckling force without impacting the behavior of the rolling joint. The rolling joint

was shown to prevent airflow below 15psi, allowing for the rolling joint to be treated as a seal for pneumatic or hydraulic actuation at lower pressures.

We discovered that there was an angle dependant linear relationship between the input pressure and the force that the mechanism can apply. The slope of this relationship changed with the configuration of the robot. In the future the force transmission capabilities of this mechanisms could be used for contact or force control, or possibly for sensing by measuring the pressure used to drive the motion of the mechanism.

Hydraulic control was demonstrated to be able to create repeatable bi-directional motion of the mechanism. This allows for motor free actuation which can have advantages in applications with restricted space or weight. The hydraulic controls were also able to create a vacuumed state for the actuator, making it extremely flexible. This flexible state allows compressed storage by folding the mechanism into a smaller form. It is possible to cycle repeatedly through the pressurized and vacuumed states, allowing the actuator to be stored in a compact space, extended when needed and then returned to compact storage when the job is done.

The actuator already shows some potential in its current state, but improvements in materials and fabrication methods would improve performance further. Replacing the duct tape

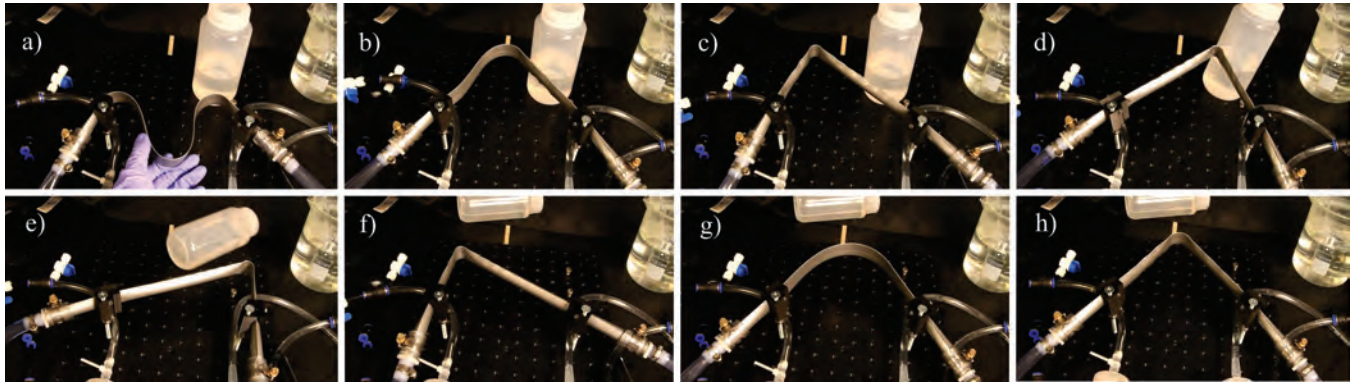


Fig. 8. Application demonstration. a) Actuator is initially vacuumed empty, making it extremely flexible. b-c) Vacuum is released and water fills the chambers, stiffening the actuator. d-e) Actuator pushes against a bottle and knocks it over. f) Actuator returns to initial position g) Fluid is pulled out of actuator, returning it to flexible vacuumed state. h) Vacuum is released and actuator regains stiffness.

wrapping with a single continuous layer of a flexible and pressure resistant material would increase the resistance to breaking and leaking along the length of the actuator. An extra rubber-like waterproof layer between the two tapes could enhance the seal formed at the rolling joint when the tapes press together. These two improvements could allow for higher internal pressures and therefore more force output.

ACKNOWLEDGMENTS

Funding support was provided through the Mechanical and Aerospace Engineering Department at UCSD. This material is based upon work supported by the National Science Foundation under Grant No. 1935324. Any opinions, findings, and conclusions or recommendations expressed in this material are those of the author(s) and do not necessarily reflect the views of the National Science Foundation.

REFERENCES

- [1] Y. Yang, Y. Qin, Y. Tang, Y. Yang, Y. Peng, and H. Pu, "Deployable closed-loop tape-spring manipulators with mobile drive components on localized folds," *Mechanism and Machine Theory*, vol. 167, p. 104553, 2022.
- [2] D. Piovesan, M. Zaccariotto, C. Bettanini, M. Pertile, and S. Debei, "Design and Validation of a Carbon-Fiber Collapsible Hinge for Space Applications: A Deployable Boom," *Journal of Mechanisms and Robotics*, vol. 8, no. 3, p. 031007, 03 2016. [Online]. Available: <https://doi.org/10.1115/1.4032271>
- [3] A. J. Cook and S. J. Walker, "Experimental research on tape spring supported space inflatable structures," *Acta Astronautica*, vol. 118, pp. 316–328, 2016. [Online]. Available: <https://www.sciencedirect.com/science/article/pii/S0094576515003872>
- [4] C. Sparks, N. Justus, R. Hatton, and N. Gravish, "Amoeba-inspired swimming through isoperimetric modulation of body shape," in *2022 IEEE/RSJ International Conference on Intelligent Robots and Systems (IROS)*. IEEE, 2022, pp. 2685–2692.
- [5] T. Ding, B. Li, H. Liu, Y. Peng, and Y. Yang, "Planar multi-closed-loop hyper-redundant manipulator using extendable tape springs: Design, modeling, and experiments," *IEEE Robotics and Automation Letters*, vol. 7, no. 3, pp. 6630–6637, 2022.
- [6] G. Aridon, D. Rémond, F. Morestin, L. Blanchard, and R. Dufour, "Self-Deployment of a Tape-Spring Hexapod: Experimental and Numerical Investigation," *Journal of Mechanical Design*, vol. 131, no. 2, p. 021003, 01 2009. [Online]. Available: <https://doi.org/10.1115/1.3042148>
- [7] J. Quan and D. Hong, "Flexible Long-Reach Robotic Limbs Using Tape Springs for Mobility and Manipulation," *Journal of Mechanisms and Robotics*, vol. 15, no. 3, p. 031009, 04 2023. [Online]. Available: <https://doi.org/10.1115/1.4062150>
- [8] B. Mosadegh, P. Polygerinos, C. Keplinger, S. Wennstedt, R. F. Shepherd, U. Gupta, J. Shim, K. Bertoldi, C. J. Walsh, and G. M. Whitesides, "Pneumatic networks for soft robotics that actuate rapidly," *Advanced functional materials*, vol. 24, no. 15, pp. 2163–2170, 2014.
- [9] B. Verrelst, F. Daerden, D. Lefeber, R. Van Ham, and T. Fabri, "Introducing pleated pneumatic artificial muscles for the actuation of legged robots: a one-dimensional setup," in *Proceedings of the 3rd International Conference on Climbing and Walking Robots*, 2000, pp. 583–590.
- [10] M. Tian, Y. Xiao, X. Wang, J. Chen, and W. Zhao, "Design and experimental research of pneumatic soft humanoid robot hand," in *Robot Intelligence Technology and Applications 4: Results from the 4th International Conference on Robot Intelligence Technology and Applications*. Springer, 2017, pp. 469–478.
- [11] S. K. Talas, B. A. Baydere, T. Altinsoy, C. Tutcu, and E. Samur, "Design and development of a growing pneumatic soft robot," *Soft Robotics*, vol. 7, no. 4, pp. 521–533, 2020, pMID: 32150509. [Online]. Available: <https://doi.org/10.1089/soro.2019.0083>
- [12] N. Wang, B. Chen, X. Ge, X. Zhang, and W. Wang, "Modular crawling robots using soft pneumatic actuators," *Frontiers of Mechanical Engineering*, vol. 16, pp. 163–175, 2021.
- [13] Q. Guan, L. Liu, J. Sun, J. Wang, J. Guo, Y. Liu, and J. Leng, "Multi-functional soft stackable robots by netting–rolling–splicing pneumatic artificial muscles," *Soft Robotics*, 2023.
- [14] Q. Tan, Y. Chen, J. Liu, K. Zou, J. Yi, S. Liu, and Z. Wang, "Underwater crawling robot with hydraulic soft actuators," *Frontiers in Robotics and AI*, vol. 8, p. 688697, 2021.
- [15] S. D. Thomalla and J. D. Van de Ven, "Modeling and implementation of the mckibben actuator in hydraulic systems," *IEEE Transactions on Robotics*, vol. 34, no. 6, pp. 1593–1602, 2018.
- [16] K. Ishibashi, M. Komagata, H. Ishikawa, O. Azami, and K. Yamamoto, "Compact water pump and its application to self-contained soft robot hand for vegetable factory," *Advanced Robotics*, vol. 37, no. 15, pp. 970–986, 2023.
- [17] A. Zatopa, S. Walker, and Y. Menguc, "Fully soft 3d-printed electroactive fluidic valve for soft hydraulic robots," *Soft robotics*, vol. 5, no. 3, pp. 258–271, 2018.
- [18] Z. M. Hammond, N. S. Usevitch, E. W. Hawkes, and S. Follmer, "Pneumatic reel actuator: Design, modeling, and implementation," in *2017 IEEE International Conference on Robotics and Automation (ICRA)*. IEEE, 2017, pp. 626–633.